

pubs.acs.org/Macromolecules Article

Controlling Architecture and Mechanical Properties of Polyether Networks with Organoaluminum Catalysts

Aaliyah Z. Dookhith, Nathaniel A. Lynd, Costantino Creton, and Gabriel E. Sanoja*



Cite This: *Macromolecules* 2022, 55, 5601–5609



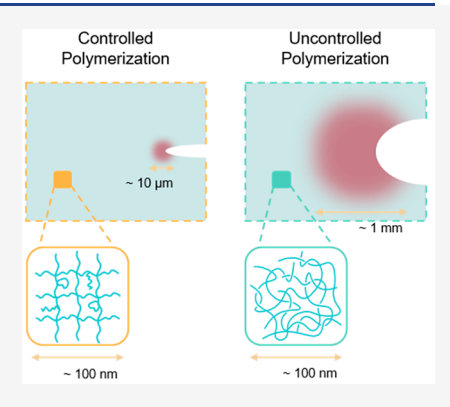
ACCESS I

Metrics & More

Article Recommendations

Supporting Information

ABSTRACT: Soft materials can sustain large, elastic, and reversible deformations, finding widespread use as elastomers and hydrogels. These materials constitute 3-D polymer networks and are typically synthesized by cross-linking polymer chains or copolymerizing monomer and cross-linker. Seminal investigations have enabled control over the network architecture by cross-linking chains of poly(dimethylsiloxane), poly(1,4-butadiene), or tetra-poly(ethylene glycol); however, as soft materials become attractive for robotics, electronics, and prosthetics, codesigning the network architecture, mechanical, and functional properties has become pressing. We investigate the relationship among reaction pathway, network architecture, and mechanical properties in poly(ethyl glycidyl ether) networks synthesized by epoxide ring-opening polymerization with two organoaluminum catalysts. The key result is that uncontrolled polymerizations yield loosely cross-linked, entangled, soft, and extensible networks, whereas more controlled polymerizations, instead, lead to highly cross-linked, stiff, and



brittle networks. Such catalytic control over network architecture and mechanical properties could enable design of novel soft, tough, and functional materials.

■ INTRODUCTION

Soft materials form an integral part of society as engineering elastomers and biomedical hydrogels because of their ability to sustain large, elastic, and reversible deformations. These materials have been of major interest since the discovery of rubber vulcanization in the 19th century, with numerous investigations focused on understanding the relationship between molecular structure and mechanical properties in elastomers like natural rubber, styrene—butadiene rubber, and filled rubber. However, as soft materials find use in emerging applications like robotics, electronics, and prosthetics, challenges in attaining satisfactory mechanical and functional properties have spurred renewed interest in understanding their structure—property relationships. ^{5–8}

Soft materials are constituted of polymer networks, 3D arrangements of polymer chains interconnected through cross-linking points. Solids at the macroscopic scale, these materials have liquidlike segmental dynamics and exhibit functional and mechanical properties dictated by the monomer—cross-linker chemistry and network architecture. Long-established molecular models on properties like elasticity, swelling, and fracture depict the network architecture as homogeneous, but in reality it is heterogeneous, ⁹ ill-defined, and pervaded by topological defects like dangling chains and loops. However, how these defects are formed during network synthesis remains abstract.

Polymer networks are typically synthesized by cross-linking polymer chains or copolymerizing monomer and cross-linker. Early investigations focused on controlling the network architecture by cross-linking poly(dimethylsiloxane) chains of narrow dispersity and well-defined molecular weight. The resulting materials enabled a better molecular understanding of mechanical properties like elasticity 10-12 and fracture, 13,14 but their architectures proved to be heterogeneous on the basis of small-angle scattering. 15-17 Networks of poly(butadiene), 18,19 poly(urethane),^{20,21} and poly(ethylene glycol)²² have been synthesized by using a similar strategy, with the latter ones being the most homogeneous²³ and also affording refinement of molecular models on elasticity, 24 swelling, 25 and fracture. 26 However, synthesizing polymer networks by cross-linking polymer chains requires multiple steps including, at the very least, the synthesis of polymer chains and post-cross-linking in the bulk or concentrated solution. As a result, this strategy can be time-intensive when codesigning the functional and mechanical properties of polymer networks by varying, for example, the chain composition.

Another strategy to synthesize polymer networks, instead, is to copolymerize monomer and cross-linker, with tunability of the functional and mechanical properties afforded by the monomer—cross-linker reactivity, initiator efficiency, solvent quality, reaction temperature, and concentration.^{27–29} The

Received: March 23, 2022 Revised: May 17, 2022 Published: June 22, 2022





simplicity of this reaction makes it ubiquitous in academic and industrial laboratories. However, the lack of architectural control, relative to the synthesis of polymer networks by crosslinking polymer chains, limits its potential for molecular design. Controlled radical polymerizations like NMP, ^{30,31} ATRP, ^{32–34} and RAFT have been used to synthesize polymer networks, and the recent review of Cuthbert et al.³⁷ details post-synthetic strategies to functionalize latent active sites and spatiotemporally control material properties. These networks are presumably more homogeneous than analogues synthesized by free radical polymerization due to the reversible activation and deactivation of polymer chain ends during monomer and cross-linker copolymerization, exhibiting delayed gelation and higher percolation thresholds. 30,31,33,3 Yet, how such control over the network architecture ultimately affects the mechanical properties, particularly at large deformations, remains unknown.

Here, we restrict our scope to polyether networks—a class of materials widely used as polymer electrolytes, gas separation membranes, and artificial tissue scaffolds because of their oxygen-rich backbone. Polyethers result from the ringopening polymerization of epoxides and, despite the abundance of commercially available monomers, are mainly used as poly(ethylene glycol) or poly(propylene glycol) chains with restricted backbone functionality. We outline a relationship among the reaction pathway, network architecture, and mechanical properties in model networks synthesized by ringopening copolymerization of ethyl glycidyl ether (EGE) monomer and 1,4-butanediol diglycidyl ether (BDGE) crosslinker using two different initiators/catalysts: a chelate of AlEt₃ with acetylacetone and water, termed the Vandenberg catalyst, and a chelate of AlEt3 with dimethylaminoethanol, termed the Lynd catalyst. By evaluating the kinetics of copolymerization by 1H NMR spectroscopy and GPC and the mechanical properties by rheology, uniaxial extension until failure, and single-edge notch crack propagation, we characterize the evolution of the network architecture with monomer conversion by fitting the molecular model of Rubinstein and Panyukov on non-linear elasticity of entangled and cross-linked networks.⁴² Finally, we provide insights into the role of network architecture on energy dissipation in the vicinity of the crack tip and fracture energy using the molecular model of Lake and Thomas.43

■ EXPERIMENTAL SECTION

Materials. Unless otherwise specified, all chemicals were used as received. Air- and moisture-sensitive reactions, outside the glovebox, were performed by using standard Schlenk-line techniques. Ethyl glycidyl ether (EGE), 1,4-butanediol diglycidyl ether (BDGE), and 2 M butylmagnesium chloride in THF were sourced from TCI; acetylacetone, anhydrous diethyl ether, 1.0 M triethylaluminum (AlEt $_3$) in hexanes, and dimethylaminoethanol from Millipore Sigma; methanol and dichloromethane from VWR; deuterated chloroform from Cambridge Isotopes; and hydrochloric acid from Fischer.

EGE (100 mL) was purified by stirring over butylmagnesium chloride (2.0 M in THF, 1 mL) for 1 h and distilling under vacuum. Caution! Butylmagnesium chloride is a pyrophoric and moisture-sensitive chemical and should be handled with appropriate care. Distilled EGE, acetylacetone, and DI water were placed in dry septum-sealed bottles, sparged with N_2 for 45 min, and transferred to a N_2 -filled glovebox.

Synthesis of the Vandenberg Catalyst. The Vandenberg catalyst was prepared by following a procedure reported by Beckingham et al. 44 A dry septum-sealed bottle equipped with a Teflon stir bar was placed in a LN₂ cold well located inside a N₂-filled

glovebox. Anhydrous diethyl ether (10 mL) and AlEt₃ (1.0 M in hexanes, 10 mL, 10 mmol, 2 equiv) were sequentially added with gastight syringes and stirred for 30 min. Caution! AlEt₃ is a pyrophoric and moisture-sensitive chemical and should be handled with appropriate care. Acetylacetone (0.51 mL, 5 mmol, 1 equiv) was then added with a gastight syringe, and the reaction was stirred for another 2 h. Finally, DI water was added (0.09 mL, 5 mmol, 1 equiv) with a gastight syringe, and the reaction was allowed to stir overnight at room temperature.

Synthesis of the Lynd Catalyst. The Lynd catalyst was prepared following a procedure reported by Rodriguez et al. 45 A dry septum-sealed bottle equipped with a Teflon stir bar was immersed in a LN2 cold well located inside a N2-filled glovebox. AlEt3 (1.0 M in hexanes, 12 mL, 12 mmol, 2.5 equiv) and dimethylaminoethanol (0.445 mL, 4.4 mmol, 1 equiv) were sequentially added with syringes and stirred overnight while allowing the cold well to equilibrate at room temperature.

The Lynd catalyst was purified by recrystallizing three times from hexanes in the LN_2 cold well to remove excess $AlEt_3$ and then decanting and drying overnight under vacuum inside the glovebox.

Polymerization of Ethyl Glycidyl Ether (EGE). Linear Polymers. Linear polymers were synthesized in a N₂-filled glovebox. EGE (99 mol %) and initiator/catalyst (1 mol %) were added to 20 mL scintillation vials and reacted on a hot plate equilibrated at 60 °C. Monomer conversion was monitored by $^1\mathrm{H}$ NMR spectroscopy, with spectra collected on reaction aliquots (50 $\mu\mathrm{L})$ dissolved in CDCl₃ (600 $\mu\mathrm{L})$ with a Bruker Avance 400 MHz spectrometer equilibrated at room temperature.

Linear polymers were terminated by dissolving the reaction mixture in dichloromethane (10 mL) and 0.1 M acidic methanol (500 μ L) and purified by washing with DI water (3 \times 20 mL) and separating the organic and aqueous phases via centrifugation for 10 min at 11 000 rpm and 21 °C. The organic phases were then concentrated by rotary evaporation at 45 °C, and the polymers were dried overnight at room temperature under vacuum. Number-average molecular weights, $M_{\rm n}$, and dispersities, D, were evaluated by gel permeation chromatography by eluting polymer solutions, previously filtered with PTFE of 0.45 μ m pore size, in Agilent PLgel 10 μ m MIXED-B and 5 μ m MIXED-C columns (200–10000000 g mol $^{-1}$ relative to polystyrene standards) using chloroform (50 ppm of amylene) at 0.5 mL min $^{-1}$ and 30 °C as the mobile phase.

Polymer Networks. Networks were synthesized via bulk polymerization of EGE. In a N_2 -filled glovebox, monomer EGE, cross-linker BDGE, and initiator/catalyst (1 mol %) were well-mixed in a 20 mL scintillation vial and subsequently transferred to a mold composed of two Teflon-covered glass plates sealed with a silicone spacer (\approx 0.1 cm thick). Polymerization was conducted in the glovebox antechamber for 6 days at 60 °C, and the resulting polymer networks were transferred outside of the glovebox for termination and purification. Typical network dimensions were $8 \times 4 \times 0.1$ cm³.

Polymer networks were terminated with a series of five washing steps. First, the networks were swollen in a solution of acidic methanol (0.1 M HCl) in DI water (40 mL, 90% v/v) for 2 h and then swollen in methanol for 2 h (4 \times 40 mL). The networks were allowed to dry first under ambient conditions for 4 h and then under vacuum at room temperature overnight. Gel fractions were determined from the mass difference between the as-polymerized and terminated networks. The aluminum concentrations of Lynd- and Vandenberg-catalyzed networks at 10 mol % BDGE are respectively 7900 and 100 ppm as measured by ICP-MS.

Rheology. Polymer networks were punch-cut into cylindrical specimens of 8 mm diameter and ≈1 mm thickness, and their rheological properties were evaluated in a Discovery HR-2 rheometer equipped with stainless steel flat plates of 8 mm diameter.

Frequency sweeps from 0.1 to 100 rad s⁻¹ at temperatures from 30 to 75 °C were performed within the linear viscoelastic regime at a strain of 1.00%. Time–temperature superposition was used to construct master curves at a reference temperature of 30 °C by using vertical and horizontal shift factors.

Uniaxial Tension. Polymer networks were punch-cut into dogbone-shaped specimens of 20 mm gauge length, 4 mm width, and \approx 1 mm thickness. These were marked with two dots of white paint and subsequently deformed at a cross-head velocity of 0.06 mm s⁻¹ (0.003 s⁻¹) with an Instron 34TM5 equipped with a 100 N load cell and a video extensometer. The resulting force—displacement curves were used to compute the engineering stress, σ_N , and stretch, λ .

Single-Edge-Notch Crack Propagation. Polymer networks were punch-cut into dog-bone-shaped specimens of 20 mm gauge length, 4 mm width, and ≈ 1 mm thickness. These were cut with a fresh razor blade to introduce a crack of ≈ 1 mm length, marked with two dots of white paint, and deformed at a cross-head velocity of 0.06 mm s⁻¹ (0.003 s⁻¹) with an Instron 34TM5 equipped with a 100 N load cell and a video extensometer. The resulting force—displacement curves were used to compute the engineering stress, σ_N , and stretch, λ .

RESULTS AND DISCUSSION

Role of Initiator/Catalyst on the Reaction Pathway. We synthesized linear polymers by epoxide ring-opening polymerization of ethyl glycidyl ether (EGE) using two different initiators/catalysts. Detailed synthetic conditions are provided in the Experimental Section, and reaction compositions and ¹H NMR spectra are summarized in the Supporting Information (Table S1 and Figure S1). The Vandenberg and Lynd catalysts (Figure 1A) lead to dramatically different rates and mechanisms of polymerization as evidenced by the evolution of monomer conversion with time (Figure 1B) and the distribution of molecular weights (Figure 1C). The polymerization of EGE with the Vandenberg catalyst is fast and uncontrolled, achieving 95% conversion in 1 day, high molecular weight ($M_n \approx 100 \text{ kDa}$), and broad dispersity ($D \sim 100 \text{ kDa}$) 8.4), whereas polymerization with the Lynd catalyst, instead, is slow and controlled, achieving 95% conversion in 6 days, target molecular weight ($M_{\rm n} \approx 10$ kDa), and narrow dispersity ($\tilde{D} \sim$ 1.6). These observations are consistent with previous investigations on epoxide ring-opening polymerizations, where Vandenberg-catalyzed polymerizations have obscure initiating and catalytic species that derive from reaction of AlEt $_3$ with acetylacetone and water, 46,47 and Lynd-catalyzed polymerizations, instead, are controlled (i.e., living) with a well-defined mono(μ -alkoxo)bis(ethylaluminum) initiating species that derives from reaction of AlEt₃ with dimethylaminoethanol. 45,48,49

To further understand the reaction pathway, we assumed that Vandenberg- and Lynd-catalyzed polymerizations were equilibrium-limited and estimated the apparent rate constants via the following first-order rate equation:

$$\frac{X - X_{\rm e}}{1 - X_{\rm e}} = {\rm e}^{-k_{\rm app}t} \tag{1}$$

where X, $X_{\rm e}$, $k_{\rm app}$, and t are respectively the monomer conversion, equilibrium conversion, apparent rate constant, and reaction time. Non-linear least-squares regressions yield $k_{\rm app} \sim O(10^{-2}~{\rm min}^{-1})$ for the Vandenberg catalyst and $k_{\rm app} \sim O(10^{-3}~{\rm min}^{-1})$ for the Lynd catalyst, where the symbol O() indicates the order of magnitude. These apparent rate constants, $k_{\rm app}$, are consistent with differences in the rate of polymerization (Figure 1B), though we note that they are also proportional to the concentration of active chain ends, which is lower for Vandenberg-catalyzed polymerizations based on the higher $M_{\rm n}$ (Figure 1C). Hence, it is likely that the difference in the propagation rate constants is more pronounced than that reflected in Figure 1B.

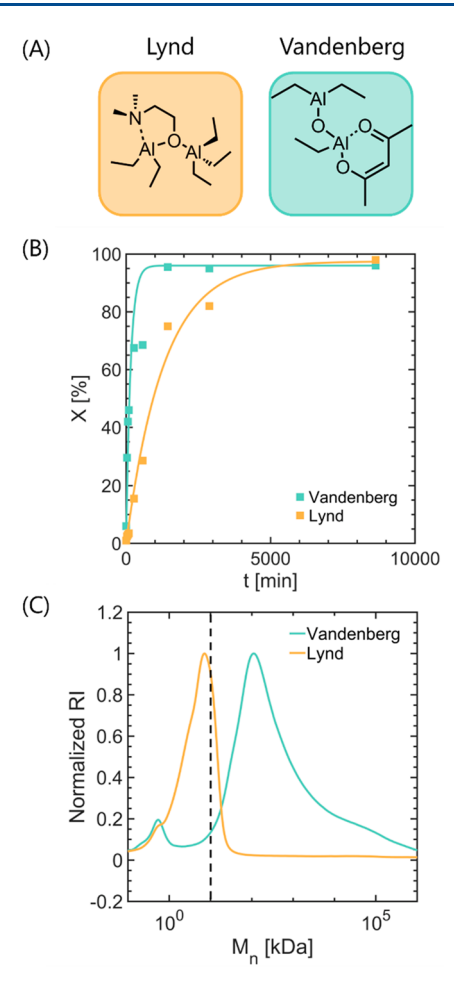


Figure 1. Polymerization of EGE with Lynd and Vandenberg catalysts. (A) Chemical structures of the Lynd and Vandenberg catalysts. (B) Evolution of monomer conversion with time demonstrates drastic differences in the rate of polymerization. (C) GPC traces unveil that Lynd-catalyzed polymerizations are controlled, attaining target molecular weight (dashed) and narrow dispersity, whereas Vandenberg-catalyzed polymerizations, instead, are uncontrolled.

We attribute differences in the rate of polymerization to the energy of the transition state, as evaluated from the temperature dependence of k_{app} using Eyring's equation:

$$\ln\left(\frac{k_{\rm app}}{T}\right) = \ln\left(\frac{k_{\rm B}}{h}\right) + \frac{\Delta S^{\ddagger}}{R} - \frac{\Delta H^{\ddagger}}{RT}$$
(2)

where T, $k_{\rm B}$, h, R, ΔH^{\ddagger} , and ΔS^{\ddagger} are respectively the temperature, Boltzmann constant, Planck constant, universal gas constant, and standard enthalpy and entropy of activation (Figures S2 and S3). Non-linear least-squares regressions yield rather similar $\Delta H^{\ddagger} \approx 20$ kcal ${\rm mol}^{-1}$ for both catalysts and comparable to that reported by Ferrier et al. for analogous allyl glycidyl ether, 47 but a lower ΔS^{\ddagger} for the Lynd catalyst (Table S2), suggesting that restrictions in the number of configurations explored by the transition state are key for attaining control over the rate of polymerization. From a molecular point of view, it is possible that more adducts of monomer and propagating chain ends are present in the transition state of Lynd-catalyzed polymerizations, reducing the number of effective collisions that lead to chain propagation and transfer/exchange reactions. However, we note that this

molecular picture remains hypothetical and requires further experimental and theoretical investigation.

The initiator/catalyst plays a key role in the rate of polymerization, molecular weight, and dispersity of the linear polymers, which is ultimately reflected in the bulk viscoelastic properties as measured by the storage G' and loss G'' moduli (Figure 2, with strain sweeps at 10 rad s⁻¹ in Figure S4).

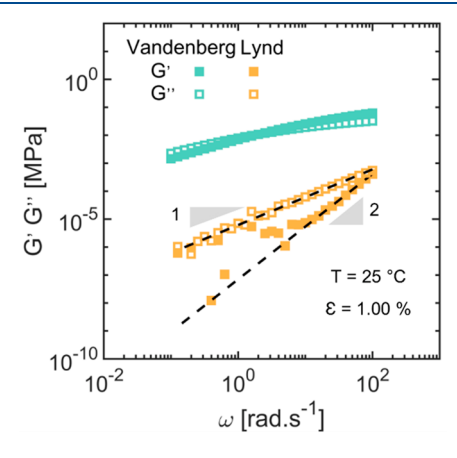


Figure 2. Linear viscoelastic properties of PEGE. Storage (\blacksquare) and loss (\square) moduli illustrate that polymers synthesized with the Vandenberg catalyst are more viscoelastic (i.e., $G' \approx G''$ or $\tan(\delta) \approx 1$) at T = 25 °C than those synthesized with the Lynd catalyst.

Vandenberg-catalyzed polymers exhibit $G' \approx G''$ and a crossover at $\omega \approx 2$ rad s⁻¹, whereas Lynd-catalyzed polymers, instead, exhibit $G'' \gg G'$ and Maxwell-like scaling $G' \sim \omega^2$ and $G'' \sim \omega$. This observation indicates that Vandenberg-catalyzed polymers are viscoelastic and able to dissipate elastic energy like entangled melts when subject to small deformations (i.e., $M_{\rm n}/M_{\rm e} \approx 3.5$, estimating an entanglement molecular weight, $M_{\rm e} \approx 30$ kDa, from rubber elasticity theory; details of this estimation are summarized in the Supporting Information), whereas Lynd-catalyzed polymers, instead, are low-molecular-weight liquids that readily flow (i.e., $M_{\rm n}/M_{\rm e} \approx 0.35$).

The initiator/catalyst inherently dictates the reaction pathway to convert monomer into polymer. Vandenberg polymerizations yield entangled melts that sustain loads and dissipate energy by molecular friction, whereas Lynd polymerizations, instead, yield low-molecular-weight polymers that readily flow like liquids. How this control over the reaction pathway affects the architecture and mechanical properties of polymer networks is the focus of the next section.

Role of the Reaction Pathway on the Network Architecture and Mechanical Properties. We synthesized polymer networks through epoxide ring-opening polymerization of EGE monomer and 1,4-butanediol diglycidyl ether (BDGE) cross-linker. Detailed synthetic conditions are provided in the Experimental Section and summarized in Table S3, but they differ in both the choice of initiator/catalyst and cross-linker concentration (Table 1).

Lynd-catalyzed networks require a higher cross-linker concentration, x=3 mol %, than Vandenberg-catalyzed networks to gel (Table S3), indirectly suggesting that the percolation threshold of EGE networks is affected by the reaction pathway and initiator/catalyst. A similar observation was interpreted by Gao et al. in networks synthesized by controlled radical polymerization within the molecular model

Table 1. Composition and Mechanical Properties of Polymer Networks: Nominal Concentration of BDGE Cross-Linker during the Polymerizationx, Density of Elastically Active Chains ν_x , Density of Entanglements ν_e , Young's ModulusE, and Fracture Energy G_c

catalyst	x (mol %) BDGE	$(10^{24} \mathrm{m}^{-3})$	$(10^{24} \mathrm{m}^{-3})$	E (MPa)	G_{c} (J m ⁻²)
Lynd	3	45	12	0.7	58
	5	150	0.82	1.6	36
	10	290	0	3.3	12
Vandenberg	3	15	6.4	0.3	130
	5	17	8.1	0.3	90
	10	18	5.8	0.3	55

of Flory and Stockmayer on gelation,³⁸ where the extent of reaction at the critical point, p_{ct} is given by

$$p_{c} = \sqrt{\frac{[M^{*}]_{t}}{2[X]_{0}}} \frac{1}{D}$$
(3)

where $[M^*]_{t}$, $[X_0]$, and D are respectively the instantaneous concentration of polymer chain ends during polymerization, the initial concentration of cross-linker, and the dispersity of the polymer chains that would result from monomer polymerization in the absence of cross-linker. These quantities can be estimated from the GPC traces of the linear polymers (Figure 1C) and the composition of the reaction mixture (Tables S3 and S4). The Flory-Stockmayer model on gelation is overly simplistic because it neglects the defective architecture of polymer networks, but it unveils, in our viewpoint, the right qualitative picture. Lynd-catalyzed networks percolate at higher cross-linker concentrations than Vandenberg-catalyzed networks because of the higher instantaneous concentration and lower dispersity of the propagating chains during copolymerization (i.e., $p_c^{\text{Vandenberg}}$ / $p_c^{\text{Lynd}} \approx 0.14$). In other words, percolation at higher crosslinker concentrations is a natural consequence of the reaction pathway that procures control over the rate of polymerization.

This effect of the reaction pathway and initiator/catalyst on network percolation is also evident in the bulk mechanical properties of the gel fraction of polyether networks (i.e., after extracting the sol fraction with organic solvent and drying in vacuum overnight; GPC trace of the sol fraction in Figure S5). Although both catalysts lead to rubbery and thermally stable materials with $T_{\rm g} \approx -55~{\rm ^{\circ}C}$ and $T_{\rm d} \approx 400~{\rm ^{\circ}C}$ (Figures S6 and S7), Vandenberg-catalyzed networks physically appear softer and tackier than their Lynd-catalyzed analogues (Figure 3A). This observation is also reflected in the viscoelastic properties, as measured by the storage G' and loss G'' moduli (Figure 3B). Vandenberg-catalyzed networks exhibit $G' \approx 0.1$ MPa at 1 Hz, frequency-dependent G'', and $G' \gg G''$, whereas Lyndcatalyzed networks, instead, exhibit $G' \approx 1$ MPa at 1 Hz and a rubbery plateau. As such, Vandenberg-catalyzed networks are softer and more dissipative (i.e., viscoelastic) than Lyndcatalyzed networks.

To further understand the role of reaction pathway on the network architecture and mechanical properties, we evaluated the mechanical properties by uniaxial elongation until failure (Figure 3C). Vandenberg-catalyzed networks are soft, extensible, and rather insensitive to the nominal concentration of BDGE cross-linker, x, whereas Lynd-catalyzed networks, instead, are stiffer, with a Young's modulus, E, that progressively increases with x. This observation agrees with

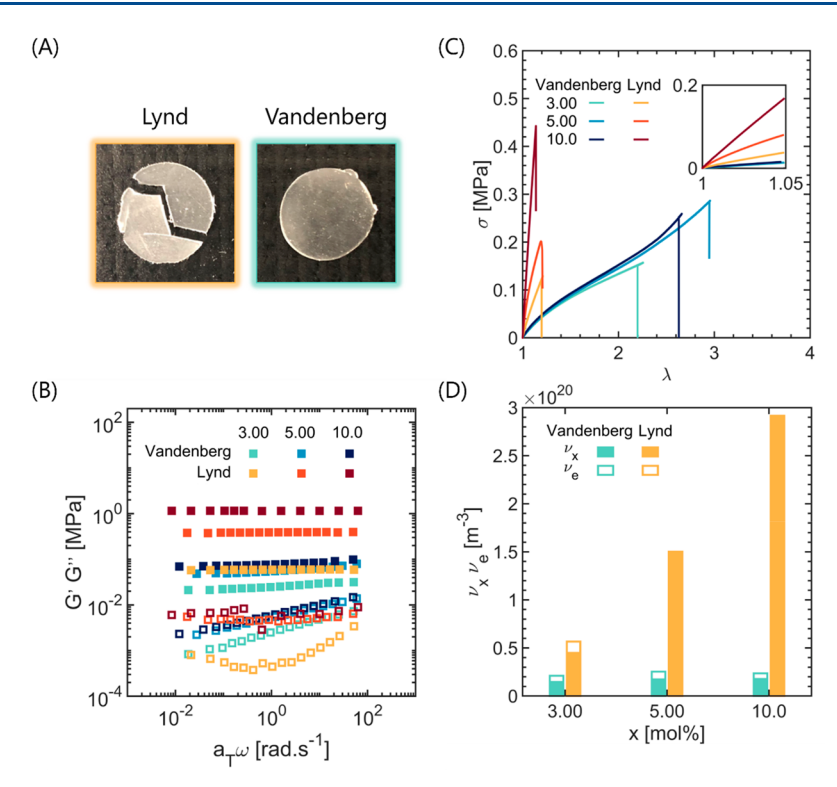
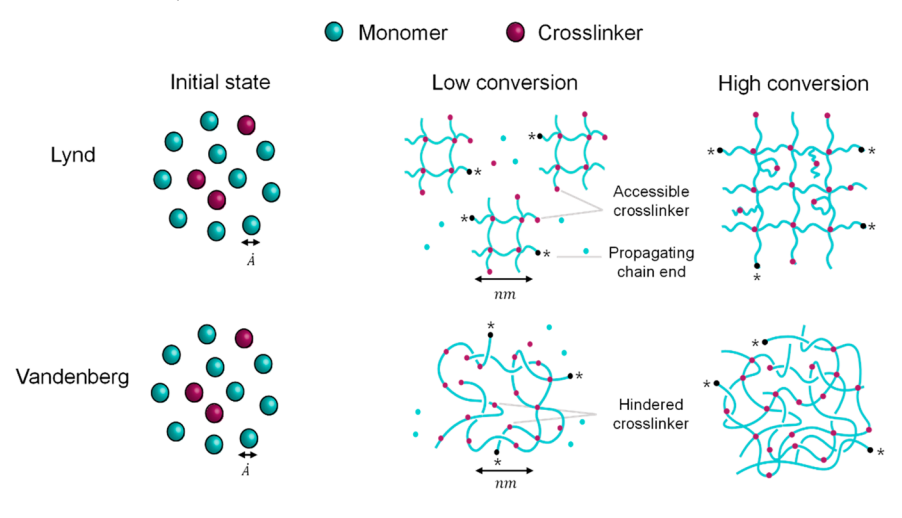


Figure 3. Mechanical properties of EGE networks. (A) Pictures of EGE $_{10}$ networks after bending. Clearly, Lynd-catalyzed networks readily crack upon bending whereas Vandenberg-catalyzed networks appear pristine. (B) Linear viscoelastic properties of EGE networks. Storage (\blacksquare) and loss (\square) moduli illustrate that networks synthesized with the Vandenberg catalyst are softer and more viscoelastic (i.e., frequency dependent G'') at T=30 °C than those synthesized with the Lynd catalyst. (C) Stress—stretch curves of EGE networks. Vandenberg-catalyzed networks are soft, extensible, and rather insensitive to the nominal concentration of BDGE cross-linker, x, whereas Lynd-catalyzed networks, instead, are stiff, with a Young's modulus, E, that progressively increases with x. (D) Densities of elastically active chains and entanglements. Vandenberg-catalyzed networks are loosely cross-linked and entangled, whereas Lynd-catalyzed networks, instead, are highly cross-linked and, a priori, untangled.

Scheme 1. Evolution of Network Architecture with Monomer Conversion: Vandenberg Polymerizations Yield Networks with Similar Densities of Entanglements and Chemical Cross-Links, whereas Lynd Polymerizations, Instead, Yield More Homogeneous Networks Pervaded by Elastic Chains



the viscoelastic response of Vandenberg-catalyzed networks, indirectly suggesting the presence of entanglements within the network architecture. The density of these entanglements, as well as that of elastically active chains, can be quantified by fitting the stress–stretch curves with the molecular model of Rubinstein and Panyukov on non-linear elasticity of entangled polymer networks (Figures S7 and S8).⁴² According to this model, the engineering stress in uniaxial tension, σ_{N} , is given by

$$\sigma_{N} = \left(\nu_{x} + \frac{\nu_{e}}{0.74\lambda + 0.61\lambda^{-0.5} - 0.35}\right) k_{B} T \left(\lambda - \frac{1}{\lambda^{2}}\right) \tag{4}$$

were λ , ν_x , and ν_e are respectively the stretch and the density of elastic chains and entanglements. Non-linear least-squares regressions reveal some important effects of the reaction pathway and initiator/catalyst on the network architecture (Figure 3D). First, the Vandenberg catalyst leads to inefficient

chemical cross-linking, likely because the reaction of a BDGE pendant epoxy moiety with a propagating chain end is limited by the entangled polymer dynamics rather than the reaction rate constant. Second, the Vandenberg catalyst leads to networks with similar densities of chemical cross-links and entanglements. And finally, control over the rate of polymerization, as attained with the Lynd catalyst, translates into effective chemical cross-linking and an increase in the modulus E with the density of elastically active chains, ν_x .

The molecular picture that results from our observations is summarized in Scheme 1. Vandenberg polymerizations lead to networks that are loosely cross-linked and entangled, whereas Lynd polymerizations, instead, yield networks that are highly cross-linked and that, a priori, appear untangled. This difference in mesoscopic heterogeneities is like that depicted for networks synthesized by controlled and free radical polymerizations, 30,31,33,34,38 though we highlight, in addition, the effect of reaction pathway on the density of elastically active chains and entanglements. Also, we note that such control over the network architecture through the initiator/ catalyst is probably related to the reactivity of the monomer and the cross-linker during polymerization, as measured by their reactivity ratios. However, this information remains experimentally inaccessible in EGE networks due to the inability to discern spectroscopic signals from EGE monomer and BDGE cross-linker during polymerization.

The initiator/catalyst serves to tailor the network architecture and linear mechanical properties like the modulus but also non-linear ones like the fracture toughness. We fractured Vandenberg- and Lynd-catalyzed networks by singleedge-notch crack propagation and estimated their critical energy release rate, G_c , following Greensmith's method (Figures S10–S12 and Table S5).⁵⁰ Irrespective of the nominal concentration of BDGE cross-linker, x, Vandenbergcatalyzed networks are tougher and more resistant to crack propagation than their Lynd-catalyzed analogues. This observation is consistent with the ability of Vandenbergcatalyzed networks to dissipate energy by molecular friction during untangling of polymer chains. Lynd-catalyzed networks, instead, are more elastic and mainly able to dissipate energy by network chain scission. Insights into the role of bond scission and molecular friction on energy dissipation can be gained by considering the critical energy release, G_c within the molecular model of Lake and Thomas. 43 According to this model, the minimum (i.e., threshold) energy dissipated upon creation of an interface, G_0 , is that required to break a monolayer of stretched elastic polymer chains and given by

$$G_0 = U_b N_x \Sigma_x \tag{5}$$

where $U_{\rm b}$, N_{x} , and Σ_x are respectively the energy of a covalent bond (i.e., typically 350 kJ mol⁻¹ but recently revised by Wang et al. to 60 kJ mol⁻¹ based on a probabilistic view of bond scission⁵¹), the number of covalent bonds between cross-links, and the areal density of elastic polymer chains. However, it is worth noting that N_x and Σ_x are coupled through

$$\Sigma_{x} \approx \frac{\nu_{x} \langle R_{0} \rangle^{1/2}}{2} \approx \frac{\nu_{x} (C_{\infty} N_{x})^{1/2} l_{0}}{2}$$
(6)

where $\langle R_0 \rangle^{1/2}$ is the average end-to-end distance of an elastic polymer chain, C_{∞} the characteristic ratio of EGE (i.e., 7.46 based on molecular dynamic simulations and comparable to that of analogous polyacetal), and l_0 the average length of a C-

C and C-O bond (i.e., 1.48 Å). As a result, the threshold energy, G_0 , is related to the density of elastic chains, ν_x , by

$$G_0 = U_b N_x \frac{\nu_x (C_\infty N_x)^{1/2} l_0}{2} \approx \frac{U_b l_0 C_\infty^{1/2}}{2} \left(\frac{\rho N_A}{M_0}\right)^{3/2} \nu_x^{-1/2}$$
(7)

where ρ , M_0 , and N_A are respectively the density of the polymer network, the molar mass of the monomer, and Avogadro's number. Equation 7 unveils a trade-off between the threshold fracture energy, G_0 , and the density of elastic polymer chains, ν_x , which has been experimentally validated in conventional elastomers⁵² and tetra-poly(ethylene glycol) hydrogels⁵³ under conditions where molecular friction is suppressed like high temperature or high solvent concentration.

Lynd-catalyzed networks are elastic and predominantly dissipate energy by chain scission, leading to better agreement between the critical energy release rate, G_c , and the threshold energy, G_0 (Figure 4B). Vandenberg-catalyzed networks,

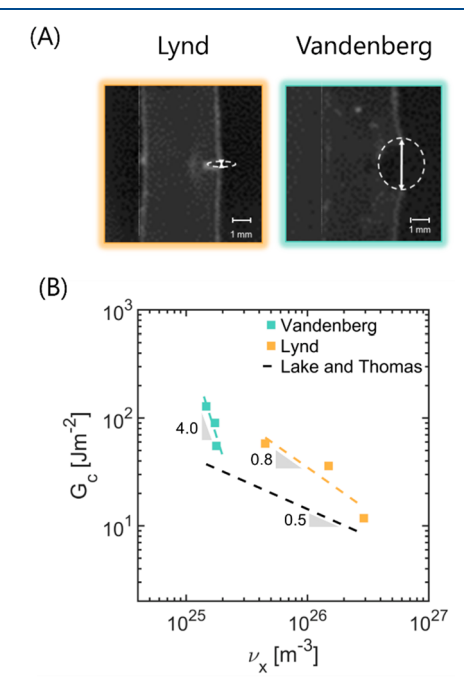


Figure 4. Fracture properties of EGE networks. (A) Pictures of EGE $_{10}$ at the critical stretch for crack propagation. Vandenberg-catalyzed networks have crack tip opening displacement, $\delta \sim O(1 \text{ mm})$, whereas Lynd-catalyzed networks, instead, have $\delta \sim O(0.1 \text{ mm})$ (Figures S13 and S14). (B) Critical energy release rate, $G_{\mathcal{O}}$ of EGE networks. Lynd-catalyzed networks exhibit better agreement with the Lake and Thomas model on fracture in terms of the scaling with ν_x .

instead, are viscoelastic and able to dissipate a notable amount of energy by molecular friction, yielding marked deviations of $G_{\rm c}$ from $G_{\rm 0}$. This difference in dissipation mechanism is also reflected in the fracture surfaces (Figure S13), which are smoother for viscoelastic, Vandenberg-catalyzed networks as in synthetic elastomers like styrene—butadiene rubber. However, we note that Vandenberg-catalyzed networks are also more blunted than Lynd-catalyzed networks at the critical point (Figure 4A), indicating that they are also subject to larger deformations ahead of the crack tip (i.e., see elastoadhesive length in Figure S14 and crack tip opening displacement at the onset of crack propagation in Figure

S15). Slootman et al. recently argued that such stretch concentration because of molecular friction also increases the local probability of bond scission, coupling the mechanisms of energy dissipation that control fracture in polymer networks. Hence, it is possible for the critical energy release rate, G_c , of Vandenberg-catalyzed networks to notably deviate from the Lake and Thomas threshold energy, G_0 , because of not only viscoelastic dissipation but also molecular damage.

Finally, it is also interesting to note that Vandenbergcatalyzed networks exhibit dramatic differences in critical energy release rate, G_{c} despite having similar densities of elastically active chains and entanglements (i.e., elastic modulus and strain softening in Figure 2C). This observation indicates that refined descriptions of the network architecture are necessary to understand energy dissipation and fracture. The molecular model of Rubinstein and Panyukov describes the non-linear behavior of entangled polymer networks up to moderate strains, but the region ahead of the crack tip, instead, is subject to large strains because the polymer chains extend near their limiting extensibility. Vandenberg-catalyzed networks synthesized with higher nominal concentrations of cross-linker strain harden at lower strains, suggesting that they are composed of less extensible chains and able to dissipate less energy by network chain scission (Figure 2C, Figure S16, and Table S6). In addition, these networks have a lower viscoelastic dissipation factor, $tan(\delta)$, at the characteristic frequency of crack propagation, indicating that they also dissipate less energy by molecular friction (Figure S17 and Table S6). Hence, increasing the nominal concentration of cross-linker in Vandenberg-catalyzed networks compromises energy dissipation by both molecular damage and friction, resulting in less resistance to crack propagation as measured by the critical energy release rate, G_c .

■ CONCLUDING REMARKS

Polymer networks synthesized by epoxide ring-opening polymerization provide novel insights into the role of reaction pathway on network architecture and mechanical properties. Fast and uncontrolled polymerization with the Vandenberg catalyst, a chelate of AlEt₃ with acetylacetone and water, yields loosely cross-linked, entangled, soft, and extensible networks, whereas slow and controlled polymerization with the Lynd catalyst, a chelate of AlEt₃ with dimethylaminoethanol, instead, results in highly cross-linked, stiff, and brittle networks. This trade-off between stiffness and elasticity at low deformations (i.e., high modulus and negligible energy dissipation) and resistance to crack propagation (i.e., high toughness) is characteristic of polymer networks that rely on molecular friction to dissipate energy in the vicinity of the crack tip.

A typical strategy to tune the architecture and mechanical properties of polymer networks is to vary the nominal concentration of cross-linker in the polymerization. However, polymerization with the Vandenberg catalyst results in networks with an elastic modulus insensitive to the cross-linker concentration, whereas polymerization with the Lynd catalyst does not afford percolated networks at cross-linker concentrations below 3 mol %. As a result, tailoring the reaction pathway through the choice of organoaluminum catalyst widens the range of synthetically accessible elastic moduli, affording additional leverage over the architecture and mechanical properties of polyether networks. Nonetheless, it is worth noting that neither the Vandenberg nor the Lynd catalyst is in absolute terms fast or controlled, suggesting that

novel initiator/catalysts for epoxide ring-opening polymerization could serve to improve the mechanical properties of polyether networks.

Effective cross-linking is attained through Lynd polymerizations, but the amount of energy dissipated upon fracture is still more than that required to break a monolayer of elastic polymer chains. Other soft materials like tetra-poly(ethylene glycol) hydrogels⁵³ and olefin-based elastomers⁵² have fracture energies that approach the threshold energy in regimes where viscoelastic dissipation is negligible. As such, it is likely that our polymer networks synthesized by Lynd polymerizations, though highly cross-linked and elastic, still contain trapped entanglements and viscoelastic dissipation ahead of the crack tip.

Network architectures that result from Vandenberg polymerizations have similar densities of elastic chains and entanglements as well as an elastic modulus and strain softening that are insensitive to the nominal concentration of cross-linker during polymerization. However, these materials exhibit dramatic differences in their resistance to crack propagation, suggesting that descriptions of the network architecture beyond that afforded by the mean-field model of Rubinstein and Panyukov might be necessary to understand energy dissipation and fracture. In this regard, combinations of experiments and theory like those recently undertaken by Arora et al.,²⁶ Lin et al.,⁵⁶ and Barney et al.⁵⁷ might prove useful to understand how the load-bearing capacity of chemical cross-links, entanglements, and topological defects evolves as polymer chains deform, untangle, and fully extend before failure.

Controlling the reaction pathway with organoaluminum catalysts affords polyether networks that are elastic at low strains but able to dissipate energy primarily by bond scission above a critical strain in the vicinity of the crack tip. Such fundamental understanding of the mechanical properties serves to molecularly design soft, tough, and durable materials for engineering applications (e.g., tires and dampers), energy conversion and storage devices (e.g., wearable electronics and ion gels), and medicine (e.g., soft prosthetics).

ASSOCIATED CONTENT

Supporting Information

The Supporting Information is available free of charge at https://pubs.acs.org/doi/10.1021/acs.macromol.2c00602.

Kinetics of polymerization of EGE, thermomechanical characterization of EGE networks, evaluation of stress—stretch curves under the molecular model of Rubinstein and Panyukov on entangled polymer networks, and fracture by single edge notch crack propagation (PDF)

AUTHOR INFORMATION

Corresponding Author

Gabriel E. Sanoja — McKetta Department of Chemical Engineering, The University of Texas at Austin, Austin, Texas 78712, United States; ⊚ orcid.org/0000-0001-5477-2346; Email: gesanoja@che.utexas.edu

Authors

Aaliyah Z. Dookhith — McKetta Department of Chemical Engineering, The University of Texas at Austin, Austin, Texas 78712, United States; Occid.org/0000-0003-4219-5515

Nathaniel A. Lynd — McKetta Department of Chemical Engineering, The University of Texas at Austin, Austin, Texas 78712, United States; orcid.org/0000-0003-3010-5068

Costantino Creton – Laboratoire Sciences et Ingénierie de la Matière Molle, ESPCI Paris, Université PSL, CNRS UMR 7615, Sorbonne Université, 75005 Paris, France; orcid.org/0000-0002-0177-9680

Complete contact information is available at: https://pubs.acs.org/10.1021/acs.macromol.2c00602

Author Contributions

Research was designed by A.Z.D. and G.E.S. Synthesis and mechanical characterization were conducted by A.Z.D., and data were interpreted by A.Z.D. and G.E.S. The manuscript was written by A.Z.D. and G.E.S. and critically revised by all authors. All authors have given final approval to the final version.

Funding

This work was funded by The University of Texas at Austin. C.C. acknowledges support from the European Research Council (ERC) under the European Union's Horizon 2020 Research and Innovation Program (Grant Agreement No. 695351-CHEMECH). N.A.L. acknowledges support for synthesis from the National Science Foundation (CHE-2004167) and the Welch Foundation (F-1904).

Notes

The authors declare no competing financial interest. *Data and Materials Availability*. All data needed to evaluate the conclusions are present in the paper and/or the Supporting Information as well as in the Texas Data Repository.

ACKNOWLEDGMENTS

A.Z.D. and G.E.S. acknowledge support and guidance from Dr. Adrianne Rosales.

REFERENCES

- (1) Gent, A. N. In Engineering with Rubber; Gent, A. N., Ed.; Carl Hanser Verlag GmbH & Co. KG: München, 2012; pp I-XVIII.
- (2) Martinez, R. V.; Glavan, A. C.; Keplinger, C.; Oyetibo, A. I.; Whitesides, G. M. Soft Actuators and Robots That Are Resistant to Mechanical Damage. *Adv. Funct. Mater.* **2014**, 24 (20), 3003–3010.
- (3) Rogers, J. A.; Someya, T.; Huang, Y. Materials and Mechanics for Stretchable Electronics. *Science* (80-.). **2010**, 327 (5973), 1603–1607.
- (4) Minev, I. R.; Musienko, P.; Hirsch, A.; Barraud, Q.; Wenger, N.; Moraud, E. M.; Gandar, J.; Capogrosso, M.; Milekovic, T.; Asboth, L.; Torres, R. F.; Vachicouras, N.; Liu, Q.; Pavlova, N.; Duis, S.; Larmagnac, A.; Voros, J.; Micera, S.; Suo, Z.; Courtine, G.; Lacour, S. P. Electronic Dura Mater for Long-Term Multimodal Neural Interfaces. *Science* (80-.). 2015, 347 (6218), 159–163.
- (5) Creton, C.; Ciccotti, M. Fracture and Adhesion of Soft Materials: A Review. *Rep. Prog. Phys.* **2016**, 79 (4), 046601.
- (6) Creton, C. 50th Anniversary Perspective: Networks and Gels: Soft but Dynamic and Tough. *Macromolecules* **2017**, *50* (21), 8297–8316.
- (7) Long, R.; Hui, C.-Y.; Gong, J. P.; Bouchbinder, E. The Fracture of Highly Deformable Soft Materials: A Tale of Two Length Scales. *Annu. Rev. Condens. Matter Phys.* **2021**, *12* (1), 71–94.
- (8) Danielsen, S. P. O.; Beech, H. K.; Wang, S.; El-Zaatari, B. M.; Wang, X.; Sapir, L.; Ouchi, T.; Wang, Z.; Johnson, P. N.; Hu, Y.; Lundberg, D. J.; Stoychev, G.; Craig, S. L.; Johnson, J. A.; Kalow, J. A.; Olsen, B. D.; Rubinstein, M. Molecular Characterization of Polymer Networks. *Chem. Rev.* **2021**, *121* (8), 5042–5092.
- (9) Bastide, J.; Leibler, L. Large-Scale Heterogeneities in Randomly Cross-Linked Networks. *Macromolecules* **1988**, 21 (8), 2647–2649.

- (10) Mark, J. E.; Sullivan, J. L. Model Networks of End-linked Polydimethylsiloxane Chains. I. Comparisons between Experimental and Theoretical Values of the Elastic Modulus and the Equilibrium Degree of Swelling. *J. Chem. Phys.* **1977**, *66* (3), 1006–1011.
- (11) Gottlieb, M.; Macosko, C. W.; Benjamin, G. S.; Meyers, K. O.; Merrill, E. W. Equilibrium Modulus of Model Poly(Dimethylsiloxane) Networks. *Macromolecules* **1981**, *14* (4), 1039–1046.
- (12) Yoo, S. H.; Yee, L.; Cohen, C. Effect of Network Structure on the Stress—Strain Behaviour of Endlinked PDMS Elastomers. *Polymer (Guildf)*. **2010**, *51* (7), 1608—1613.
- (13) Llorente, M. A.; Andrady, A. L.; Mark, J. E. Model Networks of End-Linked Polydimethylsiloxane Chains 11. Use of Very Short Network Chains To Improve Ultimate Properties. *J. Polym. Sci. Part A-2, Polym. Phys.* **1981**, *19* (4), 621–630.
- (14) Genesky, G. D.; Cohen, C. Toughness and Fracture Energy of PDMS Bimodal and Trimodal Networks with Widely Separated Precursor Molar Masses. *Polymer (Guildf)*. **2010**, *51* (18), 4152–4159
- (15) Mallam, S.; Horkay, F.; Hecht, A. M.; Rennie, A. R.; Geissler, E. Microscopic and Macroscopic Thermodynamic Observations in Swollen Poly(Dimethylsiloxane) Networks. *Macromolecules* **1991**, 24 (2), 543–548.
- (16) Mendes, E.; Girard, B.; Picot, C.; Buzier, M.; Boue, F.; Bastide, J. Small-Angle Neutron Scattering Study of End-Linked Gels. *Macromolecules* **1993**, 26 (25), 6873–6877.
- (17) Seiffert, S. Scattering Perspectives on Nanostructural Inhomogeneity in Polymer Network Gels. *Prog. Polym. Sci.* **2017**, *66*, 1–21.
- (18) Taylor, C. R.; Kan, H.; Nelb, G. W.; Ferry, J. D. Rubber Networks Containing Unattached Macromolecules. VI. Stress Relaxation in End-Linked Polybutadiene with Unattached Linear Polybutadiene. *J. Rheol.* (N. Y. N. Y). 1981, 25 (5), 507–516.
- (19) Stadler, F. J.; Pyckhout-Hintzen, W.; Schumers, J.-M.; Fustin, C.-A.; Gohy, J.-F.; Bailly, C. Linear Viscoelastic Rheology of Moderately Entangled Telechelic Polybutadiene Temporary Networks. *Macromolecules* **2009**, 42 (16), 6181–6192.
- (20) Cristiano, A.; Marcellan, A.; Long, R.; Hui, C.-Y.; Stolk, J.; Creton, C. An Experimental Investigation of Fracture by Cavitation of Model Elastomeric Networks. *J. Polym. Sci., Part B: Polym. Phys.* **2010**, 48 (13), 1409–1422.
- (21) Cristiano, A.; Marcellan, A.; Keestra, B. J.; Steeman, P.; Creton, C. Fracture of Model Polyurethane Elastomeric Networks. *J. Polym. Sci., Part B: Polym. Phys.* **2011**, 49 (5), 355–367.
- (22) Sakai, T.; Matsunaga, T.; Yamamoto, Y.; Ito, C.; Yoshida, R.; Suzuki, S.; Sasaki, N.; Shibayama, M.; Chung, U. Design and Fabrication of a High-Strength Hydrogel with Ideally Homogeneous Network Structure from Tetrahedron-like Macromonomers. *Macromolecules* **2008**, *41* (14), 5379–5384.
- (23) Matsunaga, T.; Sakai, T.; Akagi, Y.; Chung, U.; Shibayama, M. Structure Characterization of Tetra-PEG Gel by Small-Angle Neutron Scattering. *Macromolecules* **2009**, *42* (4), 1344–1351.
- (24) Zhong, M.; Wang, R.; Kawamoto, K.; Olsen, B. D.; Johnson, J. A. Quantifying the Impact of Molecular Defects on Polymer Network Elasticity. *Science* (80-.). **2016**, 353 (6305), 1264–1268.
- (25) Rebello, N. J.; Beech, H. K.; Olsen, B. D. Adding the Effect of Topological Defects to the Flory—Rehner and Bray—Merrill Swelling Theories. ACS Macro Lett. **2021**, 10 (5), 531–537.
- (26) Arora, A.; Lin, T.-S.; Beech, H. K.; Mochigase, H.; Wang, R.; Olsen, B. D. Fracture of Polymer Networks Containing Topological Defects. *Macromolecules* **2020**, *53* (17), 7346–7355.
- (27) Anseth, K. S.; Bowman, C. N. Kinetic Gelation Model Predictions of Crosslinked Polymer Network Microstructure. *Chem. Eng. Sci.* **1994**, 49 (14), 2207–2217.
- (28) Anseth, K. S.; Bowman, C. N.; Brannon-Peppas, L. Mechanical Properties of Hydrogels and Their Experimental Determination. *Biomaterials* **1996**, *17* (17), 1647–1657.
- (29) Elliott, J. E.; Bowman, C. N. Kinetics of Primary Cyclization Reactions in Cross-Linked Polymers: An Analytical and Numerical

Macromolecules Article pubs.acs.org/Macromolecules

- Approach to Heterogeneity in Network Formation. Macromolecules **1999**, 32 (25), 8621–8628.
- (30) Ide, N.; Fukuda, T. Nitroxide-Controlled Free-Radical Copolymerization of Vinyl and Divinyl Monomers. Evaluation of Pendant-Vinyl Reactivity. Macromolecules 1997, 30 (15), 4268-4271.
- (31) Ide, N.; Fukuda, T. Nitroxide-Controlled Free-Radical Copolymerization of Vinyl and Divinyl Monomers. 2. Gelation. Macromolecules 1999, 32 (1), 95-99.
- (32) Bannister, I.; Billingham, N. C.; Armes, S. P.; Rannard, S. P.; Findlay, P. Development of Branching in Living Radical Copolymerization of Vinyl and Divinyl Monomers. Macromolecules 2006, 39 (22), 7483-7492.
- (33) Gao, H.; Miasnikova, A.; Matyjaszewski, K. Effect of Cross-Linker Reactivity on Experimental Gel Points during ATRcP of Monomer and Cross-Linker. Macromolecules 2008, 41 (21), 7843-
- (34) Gao, H.; Li, W.; Matyjaszewski, K. Synthesis of Polyacrylate Networks by ATRP: Parameters Influencing Experimental Gel Points. Macromolecules 2008, 41 (7), 2335-2340.
- (35) Liu, B.; Kazlauciunas, A.; Guthrie, J. T.; Perrier, S. One-Pot Hyperbranched Polymer Synthesis Mediated by Reversible Addition Fragmentation Chain Transfer (RAFT) Polymerization. Macromolecules 2005, 38 (6), 2131-2136.
- (36) Vo, C.-D.; Rosselgong, J.; Armes, S. P.; Billingham, N. C. RAFT Synthesis of Branched Acrylic Copolymers. Macromolecules 2007, 40 (20), 7119-7125.
- (37) Cuthbert, J.; Balazs, A. C.; Kowalewski, T.; Matyjaszewski, K. STEM Gels by Controlled Radical Polymerization. Trends Chem. **2020**, 2 (4), 341–353.
- (38) Gao, H.; Matyjaszewski, K. Synthesis of Functional Polymers with Controlled Architecture by CRP of Monomers in the Presence of Cross-Linkers: From Stars to Gels. Prog. Polym. Sci. 2009, 34 (4), 317-350.
- (39) Brocas, A.-L.; Mantzaridis, C.; Tunc, D.; Carlotti, S. Polyether Synthesis: From Activated or Metal-Free Anionic Ring-Opening Polymerization of Epoxides to Functionalization. Prog. Polym. Sci. **2013**, 38 (6), 845–873.
- (40) Klein, R.; Wurm, F. R. Aliphatic Polyethers: Classical Polymers for the 21st Century. Macromol. Rapid Commun. 2015, 36 (12), 1147-1165.
- (41) Zhao, Q.; Stalin, S.; Zhao, C.-Z.; Archer, L. A. Designing Solid-State Electrolytes for Safe, Energy-Dense Batteries. Nat. Rev. Mater. **2020**, 5 (3), 229–252.
- (42) Rubinstein, M.; Panyukov, S. Elasticity of Polymer Networks. Macromolecules 2002, 35 (17), 6670-6686.
- (43) Lake, G. J.; Thomas, A. G. The Strength of Highly Elastic Materials. Proc. R. Soc. A Math. Phys. Eng. Sci. 1967, 300 (1460), 108-119.
- (44) Beckingham, B. S.; Sanoja, G. E.; Lynd, N. A. Simple and Accurate Determination of Reactivity Ratios Using a Nonterminal Model of Chain Copolymerization. Macromolecules 2015, 48 (19), 6922-6930.
- (45) Rodriguez, C. G.; Ferrier, R. C.; Helenic, A.; Lynd, N. A. Ring-Opening Polymerization of Epoxides: Facile Pathway to Functional Polyethers via a Versatile Organoaluminum Initiator. Macromolecules **2017**, *50* (8), 3121–3130.
- (46) Vandenberg, E. J. Catalysis: A Key to Advances in Applied Polymer Science. Polymeric Materials Science and Engineering, Proceedings of the ACS Division of Polymeric Materials Science and Engineering 1992, 64, 2-23.
- (47) Ferrier, R. C.; Pakhira, S.; Palmon, S. E.; Rodriguez, C. G.; Goldfeld, D. J.; Iyiola, O. O.; Chwatko, M.; Mendoza-Cortes, J. L.; Lynd, N. A. Demystifying the Mechanism of Regio- and Isoselective Epoxide Polymerization Using the Vandenberg Catalyst. Macromolecules 2018, 51 (5), 1777-1786.
- (48) Ferrier, R. C.; Imbrogno, J.; Rodriguez, C. G.; Chwatko, M.; Meyer, P. W.; Lynd, N. A. Four-Fold Increase in Epoxide Polymerization Rate with Change of Alkyl-Substitution on Mono-µ-Oxo-Dialuminum Initiators. *Polym. Chem.* **2017**, 8 (31), 4503–4511.

- (49) Imbrogno, J.; Ferrier, R. C.; Wheatle, B. K.; Rose, M. J.; Lynd, N. A. Decoupling Catalysis and Chain-Growth Functions of Mono (μ -Alkoxo)Bis(Alkylaluminums) in Epoxide Polymerization: Emergence of the N-Al Adduct Catalyst. ACS Catal. 2018, 8 (9), 8796-8803.
- (50) Greensmith, H. W. Rupture of Rubber. X. The Change in Stored Energy on Making a Small Cut in a Test Piece Held in Simple Extension. J. Appl. Polym. Sci. 1963, 7 (3), 993-1002.
- (51) Wang, S.; Panyukov, S.; Rubinstein, M.; Craig, S. L. Quantitative Adjustment to the Molecular Energy Parameter in the Lake-Thomas Theory of Polymer Fracture Energy. Macromolecules 2019, 52 (7), 2772-2777.
- (52) Bhowmick, A. K. Threshold Fracture of Elastomers. J. Macromol. Sci. Part C Polym. Rev. 1988, 28 (3-4), 339-370.
- (53) Akagi, Y.; Sakurai, H.; Gong, J. P.; Chung, U.; Sakai, T. Fracture Energy of Polymer Gels with Controlled Network Structures. J. Chem. Phys. 2013, 139 (14), 144905.
- (54) Tsunoda, K.; Busfield, J. J. C.; Davies, C. K. L.; Thomas, A. G. Effect of Materials Variables on the Tear Behaviour of a Non-Crystallizing Elastomer. J. Mater. Sci. 2000, 35 (20), 5187-5198.
- (55) Slootman, J.; Waltz, V.; Yeh, C. J.; Baumann, C.; Göstl, R.; Comtet, J.; Creton, C. Quantifying Rate- and Temperature-Dependent Molecular Damage in Elastomer Fracture. Phys. Rev. X 2020, 10 (4), 041045.
- (56) Lin, S.; Ni, J.; Zheng, D.; Zhao, X. Fracture and Fatigue of Ideal Polymer Networks. Extrem. Mech. Lett. 2021, 48, 101399.
- (57) Barney, C. W.; Ye, Z.; Sacligil, I.; McLeod, K. R.; Zhang, H.; Tew, G. N.; Riggleman, R. A.; Crosby, A. J. Fracture of Model End-Linked Networks. Proc. Natl. Acad. Sci. U. S. A. 2022, 119 (7), 2-7.

□ Recommended by ACS

Macromolecular Additives to Turn a Thermoplastic Elastomer into a Self-Healing Material

Léo Simonin, Laurent Bouteiller, et al.

JANUARY 08, 2021 MACROMOLECULES

READ 2

Tough and Degradable Self-Healing Elastomer from Synergistic Soft-Hard Segments Design for Biomechano-**Robust Artificial Skin**

Xiaochen Xun, Yue Zhang, et al.

NOVEMBER 30, 2021

ACS NANO

READ **C**

Elastomers without Covalent Cross-Linking: Concatenated Rings Giving Rise to Elasticity

Pengpeng Hu, Anne Ladegaard Skov, et al.

OCTOBER 05, 2020

ACS MACRO LETTERS

RFAD 17

Utilizing the "Dangling Group Effect" Caused by the Cross-Linked Network Topology Transformation to Prepare High-**Performance and Deformable Resins and Composites**

Ji Zhou, Mei Liang, et al.

SEPTEMBER 10, 2021

MACROMOLECULES

READ 🗹

Get More Suggestions >